Comparing Compact and Remote Deployments of a Speed-Controlled Cylinder Drive Unit on an Offshore Knuckle Boom Crane

Zhao, Wei; Bhola, Mohit

Published in:
PROCEEDINGS

Publication date:
2023

Document Version
Publisher's PDF, also known as Version of record

The 18th Scandinavian International Conference on Fluid Power, SICFP'23, May 30- June 1, 2023, Tampere, Finland

Comparing Compact and Remote Deployments of a Speed-Controlled Cylinder Drive Unit on an Offshore Knuckle Boom Crane

Wei Zhao[1] and Mohit Bhola[2]

[1]Engineering Sciences, University of Agder, Grimstad, Norway
[1]E-mail: wei.zhao@uia.no
[2]Engineering and Science, Aalborg University, Aalborg, Denmark
[2]E-mail: mobh@energy.aau.dk

Abstract

In recent years, the speed-controlled hydraulic cylinder has been gaining popularity due to its high energy efficiency, plug-and-play installation, and reduced maintenance. In low-power applications, the speed-controlled hydraulic cylinder's drive unit, containing electric motors, hydraulic pumps, accumulators, and auxiliary valves, is mounted on the cylinder, forming a compact and self-contained linear actuator called compact deployment. However, it can be infeasible for a high-power offshore knuckle boom crane to use compact deployment when the drive unit is too large. Therefore, remote deployment, which is to mount the speed-controlled hydraulic cylinder's drive unit in the machine room of the offshore knuckle boom crane and use long pipelines to connect cylinders, is proposed in this paper. A simulation study is conducted to compare the compact and remote deployments on a high-power application in system control performance and energy efficiency. In the simulation study, a 150 tons offshore knuckle boom crane model is developed based on data from a crane manufacturer. The drive units of the main and knuckle boom speed-controlled hydraulic cylinders are modeled according to commercial products. A pipeline model is developed to investigate the long pipe impact in remote deployment. An operational trajectory within the operating range and speed limits for the 150 tons offshore knuckle boom crane is developed. Simulation results show that the remote deployment consumes 5 % less power and has 30.5 % higher load capacity than the compact deployment without significantly compromising the position-tracking performance. Furthermore, in this paper, a speed-controlled hydraulic cylinder used on an 800 tons offshore knuckle boom crane, one of the highest-power offshore hydraulic machinery, is constructed with commercial products, demonstrating that the power output of the speed-controlled hydraulic cylinder is high enough for most offshore hydraulic machines.

Keywords: Speed-controlled cylinder, knuckle boom crane, pipeline, high power application

1 Introduction

In heavy-duty industries, hydraulic cylinders have many advantages over other linear actuators, such as higher force and power density, shock load protection, simpler structure, and the possibility of energy recuperation capability. As a mature technology, the valve-controlled system normally controls these hydraulic cylinders in heavy-duty hydraulic machines. However, the valve-controlled method causes low system energy efficiency due to valve throttling, e.g., up to 35 % of the total energy is consumed by the control valve throttling in a load-sensing compact excavator [1]. As a promising technology to replace the valve-controlled hydraulic cylinder, the speed-controlled cylinder (SCC) enhances energy efficiency by fundamentally removing the throttling losses and offering energy recovery capability. For example, the system energy efficiency can achieve 84.7 % by using an SCC with energy recovery capacity in [2]. A simplified diagram of an SCC is shown in Fig. 1. An SCC comprises two parts: a cylinder and a drive unit. The SCC's drive unit contains electric motors, hydraulic pumps, accumulators, and auxiliary valves. In an SCC, the hydraulic cylinder is connected to one or two fixed-displacement hydraulic pumps and an

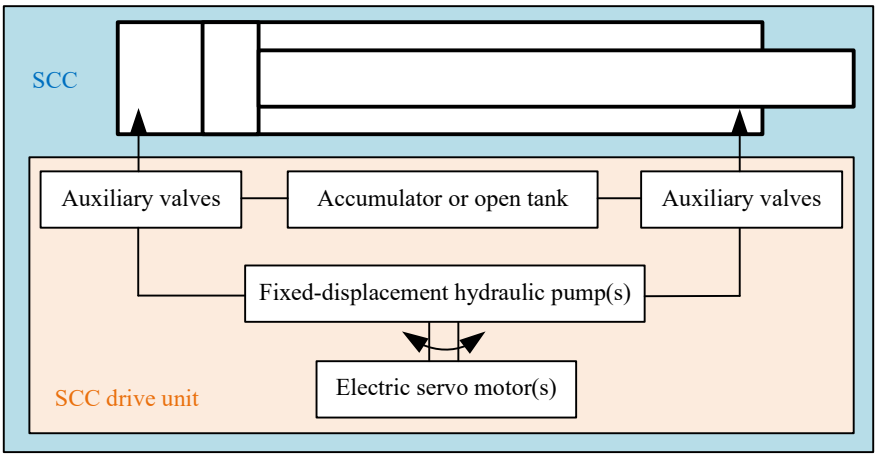

Figure 1: Structure of a speed-controlled hydraulic cylinder (SCC).

oil reservoir through auxiliary valves. The auxiliary valves are used for the differential flow rates compensation and the load-holding function. Electric servo motors drive the fixed-displacement hydraulic pumps.

In terms of how many electric motors and hydraulic pumps are used, there are mainly three types of SCC architectures in the literature: one-motor-one-pump, one-motor-two-pumps, and two-motors-two-pumps SCCs [3], [4]. One-motor-one-pump (1M1P) SCC, as shown in Fig. 2(a), was initially developed as plug-and-play and power-by-wire technology for primary flight control in the aerospace industry in the early 1990s [5], [6]. Two pilot-operated check valves (POCV) or an inverse shuttle valve (ISV) are often used to compensate for the differential flow rates in an SCC. An in-depth comparison between a 1M1P SCC crane and a load-sensing valve-controlled crane in motion control and energy efficiency was presented in [7], [8]. Simulation and experimental results showed that the 1M1P SCC has significantly better control performance, such as 75 % shorter settling time, 61 % less overshoot, 66 % better position tracking, reduction of pressure oscillations, and remarkably consumed 62 % less energy. As

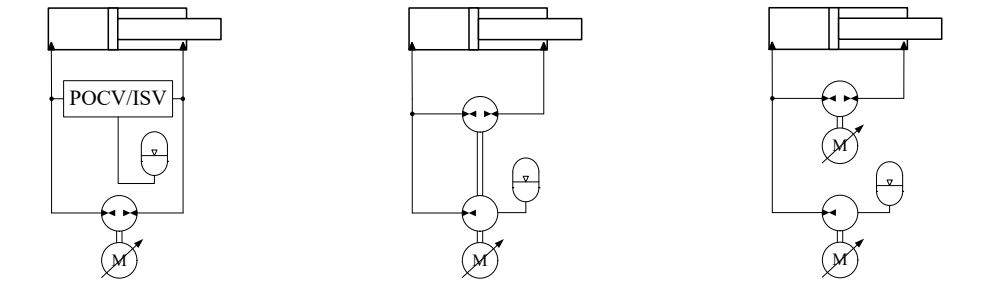

(a) One-motor-one-pump SCC. (b) One-motor-two-pump SCC. (c) Two-motor-two-pump SCC.

Figure 2: Different SCC architectures.

shown in Fig. 2(b), two hydraulic pumps driven by an electric motor are used in a one-motor-two-pump SCC. A one-motor-two-pump SCC was used to replace the valve-controlled hydraulic cylinder on a modern flight training simulator in [9]. The experimental results showed that the one-motor-two-pump SCC had the same dynamic performance as the standard valve-controlled cylinder and reduced the power consumption from 45 kW to 5 kW. Three one-motor-two-pump SCCs were implemented on an excavator model [10]. Simulation results demonstrated that the overall efficiency of this SCC excavator could achieve 73.3 % much higher than the valve-controlled excavator. As shown in Fig. 2(c), two electric motors driving two hydraulic pumps are used in a two-motor-two-pump SCC. Two-motor-two-pump SCC can increase output power for high-power level applications [11] and offer backpressure control [12]. Furthermore, in two-motor-two-pump SCC, the cylinder velocity is insensitivity to load pressure change [13]. The research on applying two-motor-two-pump SCCs on machines can be found in [14], [13], [15]. Apart from the research on SCCs in academia, several SCC commercial products made by Parker Hannifin [16], Bosch Rexroth AG [17], and Servi Group [18] have entered the market in recent years.

SCCs' drive unit, containing electric motors, hydraulic pumps, accumulators, and auxiliary valves, is mounted

on the cylinder forming a compact and self-contained linear actuator [19] in research and commercial products mentioned above. This way of installation can be called compact deployment. However, it can be problematic for high-power output multi-body hydraulic machines to use compact deployment to install the SCC's drive unit, especially when the SCC's drive unit is too large. An example of a high-power output multi-body hydraulic machine is the offshore knuckle boom crane (OKBC). A 150 tons OKBC from National Oilwell Varco is shown in Fig. 3. In this OKBC, two main boom cylinders drive the main boom, two knuckle cylinders drive the knuckle boom, and hydraulic motors realize the crane slew motion and drive the drum. Other hydraulic components, such as the HPU and control valves, are installed in the machine room. The machine room, as shown in Fig. 3, is the hydraulic machine room of the OKBC. A yoke is used when lifting tubular loads. The OKBC lifts heavy loads on drilling ships and platforms, such as drill pipes and risers. It can be seen that when an SCC drive unit is installed on the knuckle boom cylinder, the required output power of the main boom cylinder is increased to maintain the same lifting capacity. Therefore, there is a need to explore an alternative way to deploy SCCs' drive unit on OKBCs and

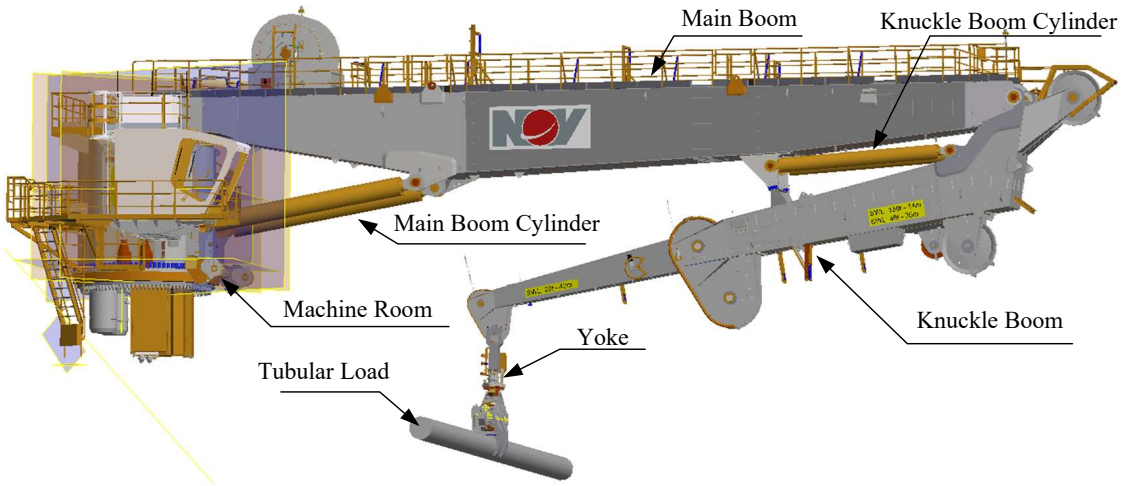

Figure 3: Inventor model of the 150 tons OKBC from National Oilwell Varco ©.

analyze the differences. Furthermore, SCCs in research and commercial products mentioned above are all at low-power or middle-power levels. Whether SCCs used on high-power level offshore applications can be constructed by off-the-shelf components has yet to be identified.

In summary, this paper makes the following novel contributions:

- Constructing a high-power SCC used on an 800 tons OKBC with sized off-the-shelf components and identifying the challenges of using compact deployment for SCC's drive unit.
- Proposing remote deployment for SCCs' drive unit on OKBCs and comparing the differences between compact and remote deployments through simulations.

The rest of this paper is formalized as follows. Constructing a 1M1P SCC for an 800 tons OKBC and mass analysis are described in Sec. 2. Modeling the mechanical and hydraulic systems are shown in Sec. 3. Simulation results are described in Sec. 4. Weak points of this paper are discussed in Sec. 5. Main conclusions and future works are shown in Sec. 6.

2 Constructing a 1M1P SCC for a 800 tons OKBC with commercial products

To answer the question of whether SCC used on large-size offshore applications can be constructed by off-the-shelf components, the 800 tons OKBC is chosen as the case study machine. It is one of the most powerful offshore applications using hydraulic cylinders [20]. From the previous work done by researchers [21] and data received from industry partners, it is observed that the maximum load acting on the main boom and knuckle boom cylinders of OKBCs are 5 and 4 times the maximum load capacity, respectively. The same ratio is used for calculating the maximum loads acting on the knuckle boom and main boom cylinders of the 800 tons OKBC. Therefore, the maximum loads acting on the main boom and knuckle boom cylinders are 4000 tons and 3200 tons, respectively. Furthermore, the cylinder speed and working pressure limits of a 150 tons OKBC are given by the industrial partner National Oilwell Varco. These limits and the maximum loads are used to calculate the cylinders' size and

select other components. Moreover, the knuckle boom cylinder is usually operated in more complicated working conditions, which will be explained in Sec. 3.3.3, than the main boom cylinder. Therefore, only the selection of off-the-shelf components for realizing the knuckle boom 1M1P SCC on the 800 tons OKBC is described in this section. After calculations, the parameters of the knuckle boom cylinder on the 800 tons knuckle boom crane are shown in Tab. 1.

Table 1: Parameters of the knuckle boom cylinder on the 800 tons knuckle boom crane

Cylinder Type	Bore Diameter [mm]	Rod Diameter [mm]	Speed Extending out [mm/s]	Speed Extending in [mm/s]	Length [m]
Knuckle Boom	1009	776	25	18	7

The major components required for the 1M1P SCC, as shown in Fig. 4, are a hydraulic pump, an electric motor, an accumulator, and a hydraulic manifold containing auxiliary valves.

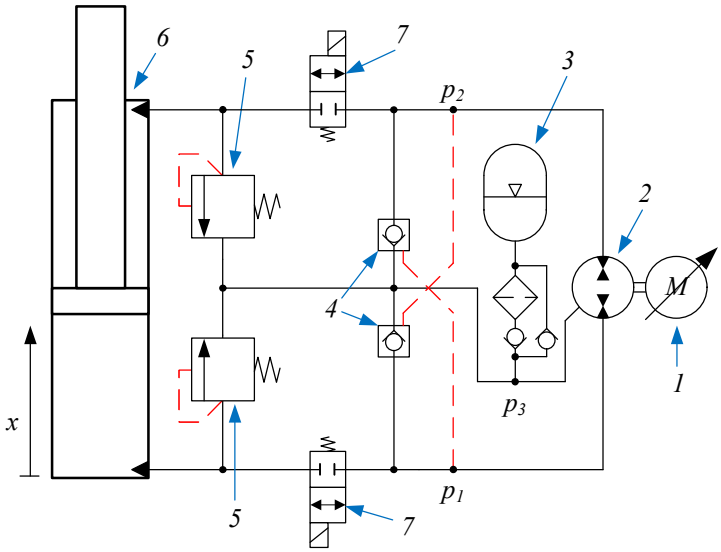

Figure 4: 1M1P speed-controlled cylinder. 1. Electrical motor, 2. Fixed-displacement hydraulic pump, 3. Accumulator, 4. Pilot-operated check valve, 5. Relief valve, 6. Single-rod hydraulic cylinder, 7. load-holding valves. p_1 is the piston side pressure, p_2 is the rod side pressure, and p_3 is the accumulator pressure.

2.1 Size of hydraulic pump and accumulator

The pump size is estimated based on the maximum speed requirements of the knuckle boom cylinder, as shown in Tab. 1.From Eq. 1, the required displacement D_p of the pump is calculated as per the data given in Tab. 1.

$$\dot{x}A_a = \omega_p \alpha_p D_p \tag{1}$$

The flow Q_{acc} from the rod side of the cylinder is shown by Eq. 2. The difference in flow due to the differential area has to be compensated by the accumulator to avoid cavitation in the pump suction side, and the required gas volume V_o is shown by Eq. 3 [22].

$$Q_{acc} = (1-\alpha)\omega_p \alpha_p D_p \tag{2}$$

$$V_o = \frac{Q_{acc} L}{\left(\frac{P_o}{P_2}\right)^{1/1.1}\left(\left(\frac{P_2}{P_1}\right)^{1/1.4} - 1\right) V_e 60} \tag{3}$$

The estimated size of the pump comes out to be 1500 cc/rev operating at the speed of 1600 rpm. However, the maximum available size of the pump manufactured by the Bosch Rexroth A4VSO model is 1000 cc/rev [23]. Hence, two pumps with 1000 cc/rev and 500 cc/rev are selected and connected on the same shaft for practical realization. Tab. 2 shows the parameters required for estimating the volume of accumulator required. Tab. 3

Table 2: Parameters for estimating required accumulator volume for flow compensation

Parameter	Denotation	Value	Unit
P_o	Pre-charge Pressure	3.6	bar
P_2	Min. working Pressure	4	bar
P_1	Max. working Pressure	11	bar

Table 3: Size of hydraulic and electric components of Knuckle boom cylinder

Designation	Denotation	Size	Unit	Mass [kg]
D_p	Displacement of Pump	1500	cc/rev	979
ω_p	Speed of electric motor	1600	rpm	10000
V_o	Gas volume of accumulator	30000	L	16000
	Variable Frequency Drive	2	MW	4830

shows the major hydraulic components for the 1M1P SCC. The minimum working pressure at the suction is considered to be 3 bar, and the accumulator volume required is 30000 L considering the effect of the temperature variations of about 20°C and margin for safety for avoiding lower pressure during the dynamic working condition. Approximately 66 accumulators of 450 L each are required for the realization of 30000 L volume [24].

2.2 Size of electric motor and manifold

The required power of the electric motor is estimated based on the required torque at the pump shaft based upon the pump's maximum operating pressure and displacement, as shown in equation 4. As mentioned above, the maximum operating pressure of the main pressure relief valve is set at 250 bar.

$$(p_a - p_b)D_p = \frac{\tau_p}{\eta_m} \tag{4}$$

Hence, at the maximum working displacement of the pump and lumped efficiency/load factor η_m of 0.65, the required power of the PMSM motor for an operating speed of 1600 rpm needs to be around 1.5 MW, and regenerative drive comes out to be of 2 MW. The mass of all the major components is shown in Tab. 2. The size of the hydraulic manifold is to be selected per the required number of paths and the cavity for the valves. The mass of the manifold is considered to be 4000 kg.

2.3 Challenges of using 1M1P-SCC on 800 tons OKBC

Regarding the above calculations and selected components for the realization of the knuckle boom 1M1P-SCC used on the 800 tons OKBC, it is confirmed that a 1M1P SCC with 3200 tons load capacity used on large-size offshore applications can be constructed by off-the-shelf components.

However, it is observed that the total mass of the knuckle boom 1M1P SCC drive unit is around 30 tons. Since the knuckle boom cylinder is mounted between the main and knuckle booms, as shown in Fig. 3, the big mass of the knuckle boom 1M1P SCC drive unit may increase the power consumption of the main boom cylinder and reduce the crane load capacity in compact deployment. To overcome these potential shortcomings in compact deployment, remote deployment, which is to mount the SCC's drive unit in the machine room of the OKBC and use long pipelines to connect cylinders, is proposed. A simulation study is conducted in Sec. 3 and 4 to investigate the system performance of remote deployment. In the simulation study, a 150 tons OKBC model from an industrial partner is used. Components of SCCs used on the 150 tons OKBC are selected using the same method described for the 800 tons OKBC. The SCC's drive unit mass of 6258 kg is added to the knuckle boom cylinder in the compact deployment simulation. A 30 m long pipeline is modeled and used in remote deployment simulation.

3 Modeling of a speed-controlled OKBC and path planning

3.1 Modeling the 150 tons OKBC

The Inventor model of the crane shown in Fig. 3 is supplied by National Oilwell Varco. The crane model consists of nine parts: a machine room, the main boom, the knuckle boom, two main boom cylinders (MBC), two knuckle boom cylinders (KBC), a tubular yoke, and a tubular payload. The key parameters of each part are listed in Tab. 4.

The dependency between load capacity and working radius is shown in Tab. 5. Nine crane parts are imported into Simscape separately and assembled as a crane dynamic Simscape model. This dynamic Simscape model will be used to connect with the Simulink model of the hydraulic drive in simulations.

Table 4: Key parameters of each part.

Parts	Length [m]	Mass [kg]
Machine Room	-	57100
Main Boom	26.1	57000
Knuckle Boom	17.8	26300
Main Boom Cylinder	5.0	8900
Knuckle Boom Cylinder	4.2	4200
Yoke	3.7	2400
Tubular Load	10	20000

Table 5: The dependency between load capacity and working radius.

Working Radius [m]	14	35	40
Load Capacity [kg]	150000	45000	20000

3.2 Modeling the 1M1P SCC

A block diagram of the 1M1P SCC used for simulations is shown in Fig. 4. An electrical motor drives a fixed-displacement hydraulic pump. The inlet and outlet of the pump are connected to the two sides of the cylinder through load-holding valves. The accumulator works as a low-pressure tank. Two pilot-operated check valves compensate for the differential flow rates from the single-rod hydraulic cylinder. High-pressure oil will be bled to the accumulator through relief valves when the cylinder receives shock loads. The modeling procedure of the main components is described in this section.

3.2.1 Electric motor

Because the main goal of the simulation is to show how the weight of SCC affects the power output of the 150 tons knuckle boom crane in different layouts, the electric motor is modeled as an angular speed source. The dynamic of this motor is represented by a first-order transfer function shown in Eq. 5. The energy efficiency aspect of the electric motor is neglected.

$$\frac{n_m}{n_{comd}} = \frac{1}{T \cdot s + 1} \tag{5}$$

3.2.2 Fixed-displacement hydraulic pump

The fixed-displacement hydraulic pump is the hydraulic power source in the circuit. Because it is rigidly connected to the electric motor, it has the same angular speed as the electric motor. The pump's dynamic is combined with the electric motor's dynamic and represented by Eq. 5. The pump flow rate is modeled by Eq. 6. The energy efficiency aspect of the hydraulic pump is neglected.

$$Q_p = V_p \cdot n_m \tag{6}$$

3.2.3 Oil bulk modulus

The bulk modulus of hydraulic oil is normally assumed to be a constant. However, it is a variable in the real world that changes depending on the chamber pressure and the relative volume of the air entrapped in the oil. This dependency is modeled by Eq. 7, 8, and 9.

$$\beta_{chb,air} = p_{chb} \cdot k_{air} \tag{7}$$

$$V_{chb,\%air} = V_{atm,\%air} \cdot \left(\frac{p_{atm}}{p_{chb}} \right)^{\frac{1}{k_{air}}} \tag{8}$$

$$\beta_{chb} = \frac{1}{\frac{1}{\beta_{oil}} + \frac{V_{chb,\%air}}{\beta_{chb,air}}} \tag{9}$$

3.2.4 Hydraulic cylinder

A hydraulic cylinder model consists of four parts: pressure build-up, pressure-force conversion, stroke limits, and cylinder friction. Pressure build-ups on the piston side and rod side of the cylinder are modeled by by Eq. 10 and Eq. 11.

$$\dot{p}_1 = \frac{\beta_{chb} \cdot (Q_{pis} - v_{rod} \cdot A_{pis})}{V_0 + x_{rod} \cdot A_{pis}} \tag{10}$$

$$\dot{p}_2 = \frac{\beta_{chb} \cdot (v_{rod} \cdot A_{annu} - Q_{rod})}{V_0 + (x_{end} - x_{rod}) \cdot A_{annu}} \tag{11}$$

The pressure-force conversion is modeled as Eq. 12.

$$F_{cyl} = p_1 \cdot A_{pis} - p_2 \cdot A_{annu} \tag{12}$$

The cylinder stroke ends are modeled as a contact force shown in Eq. 13.

$$F_{cont} = (x_{rod} - x_{lim}) \cdot k_{cont} + v_{rod} \cdot c_{cont} \tag{13}$$

The friction between the rod and the cylinder is modeled by the Stribeck friction shown in Eq. 14.

$$F_f = f_v \cdot v_{rod} + \tanh(\gamma \cdot v_{rod}) \cdot \left(F_C + F_S \cdot e^{\frac{-v_{rod} \cdot \tanh(\gamma \cdot v_{rod})}{\tau}} \right) \tag{14}$$

3.2.5 Pressure relief valve

Pressure relief valves are modeled by Eq. 15 and Eq. 16.

$$Q_{rv,pis} = (p_1 - p_3 - p_{crk,rv}) \cdot k_{rv} \tag{15}$$

$$Q_{rv,rod} = (p_2 - p_3 - p_{crk,rv}) \cdot k_{rv} \tag{16}$$

3.2.6 Pilot-operated check valve

Pilot-operated check valves (POCV) compensate for the differential flow rates caused by different areas on two sides of the cylinder. POCVs are modeled as variable-opening orifices. Flow rates passing through POCVs are calculated by Eq. 17 and 18.

$$Q_{pocv,pis} = C_d \cdot u_{pocv,pis} \cdot A_{pocv} \cdot \sqrt{\frac{2 \cdot |p_1 - p_3|}{\rho}} \cdot sign(p_1 - p_3) \tag{17}$$

$$Q_{pocv,rod} = C_d \cdot u_{pocv,rod} \cdot A_{pocv} \cdot \sqrt{\frac{2 \cdot |p_2 - p_3|}{\rho}} \cdot sign(p_2 - p_3) \tag{18}$$

POCV opening commands are calculated by Eq. 19 and 20 and POCV valve dynamic is modeled by Eq. 21.

$$u_{comd,pis} = \frac{p_3 + p_2 \cdot \Psi - p_{crk,pcv} - p_1}{k_{pocv}} \tag{19}$$

$$u_{comd,rod} = \frac{p_3 + p_1 \cdot \Psi - p_{crk,pocv} - p_2}{k_{pocv}} \tag{20}$$

$$\frac{u_{pocv}}{u_{comd}} = \frac{\omega_{pocv}^2}{s^2 + 2 \cdot \zeta_{pocv} \cdot \omega_{pocv} \cdot s + \omega_{pocv}^2} \tag{21}$$

3.2.7 Load-holding valves and accumulator

Because the main goal of the simulation is to show how the weight of SCC affects the power output of the 150 tons knuckle boom crane in different layouts, the load-holding function is not investigated in the simulation. Therefore, load-holding valves are neglected in the SCC model.

The accumulator stores oil when the cylinder retracts and supplies oil when the cylinder extends. Therefore, it is modeled as a low-pressurized reservoir.

3.2.8 Long pipeline modeling

As discussed in Sec. 2, it requires long pipelines of about 30 m in remote deployment. Hence to investigate the effect of a long pipeline on the response and energy losses, the dynamic model and turbulent pipe loss model as a lumped system are studied [25]. The dynamic model of the pipeline using lumped parameter approximation is shown in Fig. 5.

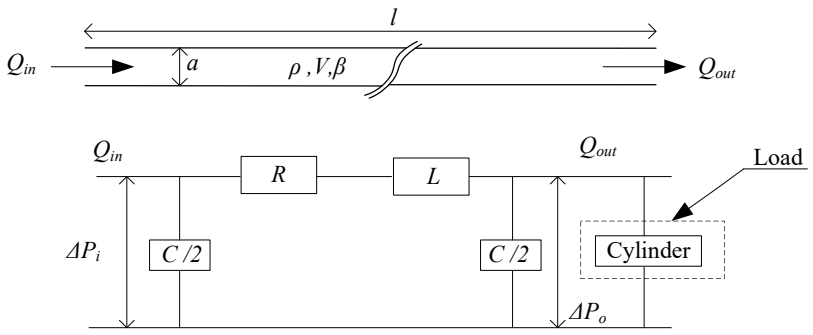

Figure 5: Line dynamics model with Lumped parameter approximation

The L, C, and R are the hydraulic inductance, capacitance, and resistance of the transmission line, which are shown by equations 22, 23, and 24.

$$R = \frac{\Delta P_o - \Delta P_i}{Q_{in}} \tag{22}$$

$$L = \frac{\rho l}{a} \tag{23}$$

$$C = \frac{V}{\beta} \tag{24}$$

The linear transfer function model of the pipeline is shown below in Eq. 25.

$$\frac{Q_o(s)}{Q_i(s)} = \frac{1}{1 + \frac{CR}{2}s + \frac{LC}{2}s^2} \tag{25}$$

In the turbulence model for estimating the pressure loss, the inner diameter is 50 mm, the maximum flow rate is 660 L/min, and the Reynolds number is greater than 5000. The following Tab. 6 shows the value used for estimating the long pipeline dynamics model. The natural frequency for the line system is $\omega_n = \sqrt{\frac{2}{LC}}$, which is 55 rad/s.

Table 6: Parameters used for estimating the linear lumped dynamic model for long pipeline

Parameter	Value	Unit
Line Resistance (R)	$2.5 \cdot 10^7$	Ns/m^2
Line Inductance (L)	$1.3 \cdot 10^7$	kg/m^4
Line Capacitance (C)	$4.9 \cdot 10^{-7}$	m^5/N

3.3 Path planning

3.3.1 Crane operation trajectory

When the 150 tons OKBC is used to move heavy tubular loads on the deck, it normally involves lifting up, translational moving, and lifting down. The operation must be within the crane operating range, shown as the blue curve in Fig. 6. Therefore, the operating trajectory is planned to start from coordinate (17.5 m, -10 m) to (32.5 m, -10 m) and horizontally pass through two points with the height of 15 m. The height of the deck is assumed at -10 m. After using the spline function to remove sharp corners, the planned trajectory can be seen as the red curve in Fig. 6.

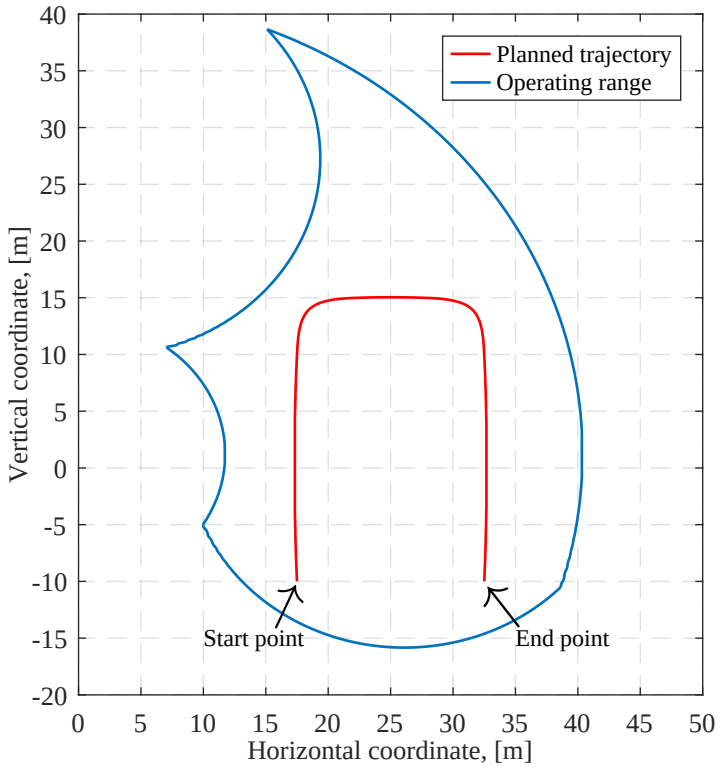

Figure 6: Planned trajectory within crane operating range.

3.3.2 Cylinder inputs and velocity limits

The planned payload trajectory is fed to the crane Simscape model described in Sec. 3.1 to get the reference input signals for the MBC and KBC. Furthermore, according to the safety design requirement from National Oilwell Varco, there are velocity limitations for the main boom and knuckle boom cylinders. These limitations are shown in Tab. 7. According to cylinder velocity plots shown in Fig. 7 and 8, MBC and KBC velocities are all within the limitations.

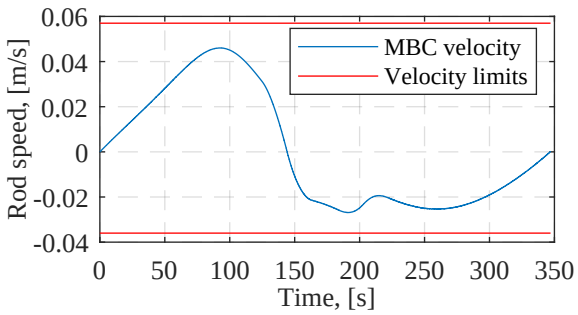

Figure 7: MBC velocity and limits.

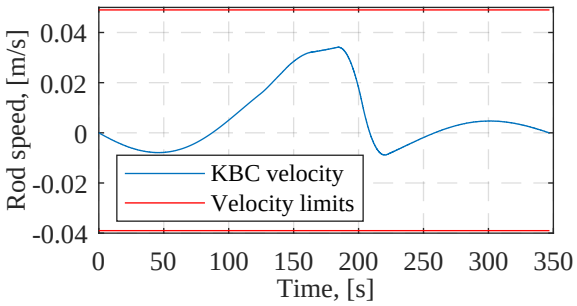

Figure 8: KBC velocity and limits.

Table 7: Cylinder speed limitations.

Parts	Stroke Out [m/s]	Stroke In [m/s]
Main Boom Cylinder	0.057	0.036
Knuckle Boom Cylinder	0.049	0.039

3.3.3 Four-quadrant operation on KBC

Which quadrant a cylinder is operated in is determined by the cylinder velocity $\dot{x}$ and cylinder force F_C [26]. As shown in Fig. 10, when $\dot{x}$ and F_C are in the same direction, the cylinder is operated in quadrant 1 and 3; when they are in different directions, the cylinder is operated in quadrant 2 and 4. The red color represents high pressure, and the blue represents low pressure.

MBC and KBC forces used to drive the crane following the operation trajectory are shown in Fig. 9. It can be seen that the MBC force is always positive, and the KBC force is negative before 94.3s and positive after 94.3s. As shown in Fig. 8, the MBC velocity changes from positive to negative at 145s, and the KBC velocity crosses zero three times at 87.0s, 208.5s, and 258.3s. Therefore, along the developed trajectory, the MBC is operated in two quadrants: 1 and 4, and the MBC rod side is always connected to the accumulator. The KBC is operated in four quadrants.

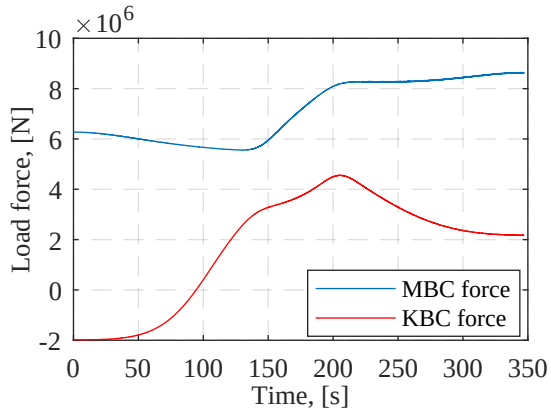

Figure 9: MBC and KBC forces.

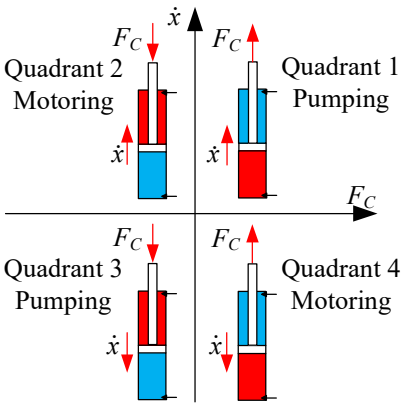

Figure 10: Demonstration of four-quadrant operation.

4 Simulation results

The MBC is connected to the machine room. Therefore, whether in compact or remote deployment, the weight of the MBC SCC drive unit does not significantly influence the MBC pressure, and only a short pipeline is needed to connect the main boom SCC drive unit and the MBC in the latter case. Hence, the difference between the main boom SCC drive unit using compact and remote deployment is neglected. The main difference between compact and remote deployment in simulations is the effect of the KBC SCC's drive unit when using compact deployment and the long pipeline connection when using remote deployment.

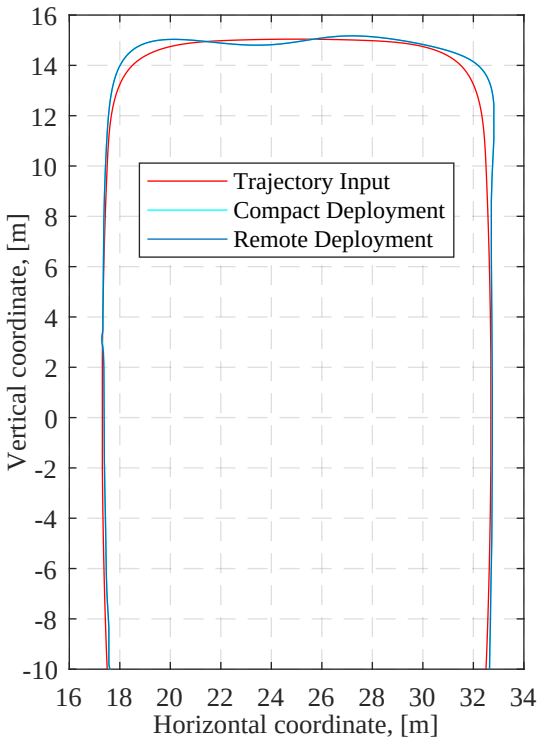

Figure 11: Payload position outputs.

4.1 Position tracking results

The crane payload position outputs for compact and remote deployments are shown in Fig11. It can be seen that payload position outputs in compact and remote deployment are overlapped, provided that the same PID controller was used in two simulations. Therefore, the remote-deployed SCC has a similar position-tracking performance as the compact-deployed SCC, and the long pipeline dynamic transfer function described in Sec. 3.2.8 does not affect the system control performance. The maximum position tracking error is around 1.5 m on corners, around 0.1 m in vertical lifting, and around 0.2 m in horizontal moving.

4.2 Pressure and power differences in two deployments

Because the MBC is so close to the machine room, the pipeline connection for the MBC SCC drive is neglected. Therefore The MBC SCC pump pressures are identical to the cylinder pressures. As described in Sec. 3.3.3, the MBC is operated in quadrants 1 and 4, and the MBC rod side is always connected to the accumulator. Therefore, the MBC rod side pump pressure is always around 3 bar in the two deployments. The MBC piston side pump pressure differences in the two deployments are shown in Fig. 12. It can be seen that there is a significant difference between the two deployments. When the KBC SCC is in compact deployment, the weight of the SCC's drive unit becomes an extra load applied on the MBCs while the load applied on the KBCs stays the same. Therefore, the MBC piston side pump pressure is lower when the KBC SCC's drive unit is in remote deployment. After calculation, this pressure is reduced by 5.1 % to 6.2 % along the simulation trajectory.

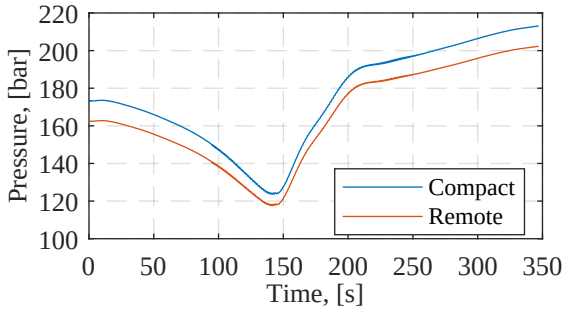

Figure 12: MBC piston side pump pressure.

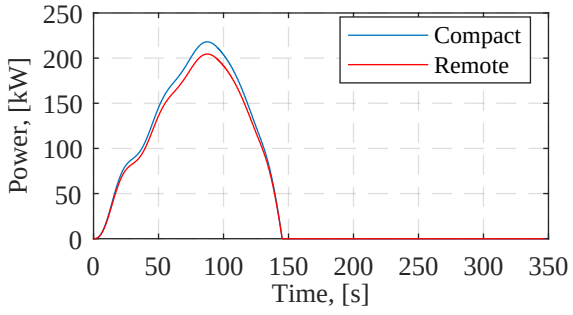

Figure 13: Main boom cylinder piston side power.

Because the flow rates on two sides of the MBC are the same in the two deployments and the rod side pressure is the same as the accumulator pressure, the MBC SCC pump power is proportional to the piston side pressure. Therefore, the MBC SCC pump power is reduced by 5.1 % to 6.2 % in remote deployment. The MBC SCC pump power for two ways of deployment are shown in Fig. 13. Because the energy recuperation under the assistant load is not considered in this paper, the MBC SCC pump power is zero after 145s. The peak power appears at 87.5s. The MBC peak pump power in compact deployment is 218.0 kW, and in remote deployment is 204.5 kW. The pump peak power is reduced by 13.5 kW. Therefore, 6.2 % peak power can be saved in remote deployment. After increasing the tubular load from 20 tons to 26.1 tons (30.5 %) in remote deployment, the MBC SCC pump power reaches the same level as the one in compact deployment.

4.3 Pipeline losses

Two long pipelines are used to connect the SCC's drive unit and the KBC in remote deployment. As described in Sec. 3.2.8, the pipeline causes a pressure drop. In simulations, the peak pressure drop on the KBC piston side is 1.1 bar, and on the rod side is 0.25 bar. These small pressure drops are negligible. Therefore, the KBC pressures are almost the same in two deployments. Power losses caused by long pipelines on the KBC piston and rod sides are shown in Fig. 14.

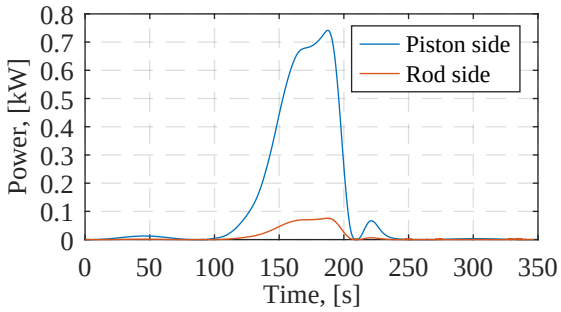

Figure 14: KBC rod side pipeline power losses.

The maximum power loss on the piston side is 0.75 kW, and on the rod side is 0.08 kW. These peak values appear from the 150s to the 200s. It is because the KBC has the maximum rod speed in this period, as shown in Fig. 8. Because the KBC rod side is connected to the accumulator from the 150s to the 200s, the KBC rod side pipeline power loss is much smaller. The total pipeline peak power loss is 0.4 % of the SCC pump peak output power.

5 Discussion

The main goals of this paper are to identify the upper power limit of SCC used on OKBCs and numerically analyze the output power difference between the two ways of deploying the SCC drive on OKBCs. Concerning the modeling in this paper, high-power electric motors have large inertia causing slow response. Therefore, the electric motor in the SCC model is simplified as a first-order transfer function with a 2s time constant. This simplification is acceptable when investigating the output power and system pressure. A more detailed electric motor model, including motor dynamics and electromagnetic conversion, is needed when researching system controls. The electric motor and hydraulic pump energy losses are not modeled since they are the same for the two options. However, when investigating the whole system's energy efficiency, the electric motor and hydraulic pump's energy efficiencies must be modeled. The low-pressure accumulator is modeled as a low-pressure source for simplicity. Even though a detailed accumulator model can offer more precise simulation results, it does not contribute to comparing the output powers between the two ways of deployment. Referring to section 3.3.3, the pipeline dynamics model is implemented in the simulation model to study its effect. It is observed that due to non aggressive cylinder speed requirements and slow response of electric motor due to heavy inertia makes the system with high damping hence the effect of line dynamics is significant as shown by simulation results. Therefore, it is recommended to install the hydraulic components at the machine room for heavy cranes which results in increase in energy efficiency of the crane operation with lower throttling losses.

Regarding SCC's maintenance for large OKBCs, remote deployment is superior to compact deployment. Large OKBCs use long cylinders to drive long booms. In compact deployment, the KBC SCC drive is far from the deck and the machine room, which causes difficulties in regular maintenance, e.g., changing the oil and regularly checking and troubleshooting rotational components. In remote deployment, because all key SCC components are

installed in the machine room, it is easier to conduct regular maintenance. High-power SCCs contain large electric motors and accumulators. Therefore, the SCC drive size is much bigger than the cylinder. As shown in Fig. 3, when the KBC is fully retracted, there might be no room for the high-power SCC drive around the cylinders. Furthermore, OKBC manufacturers can easily replace the valve-controlled drive installed in the machine room with the SCC drive using remote deployment without redesigning the mechanical part of the crane.

6 Conclusion and future works

6.1 Conclusion

A literature survey emphasized the need to identify the upper power limit of SCC used on OKBCs. After constructing the high-power SCC with existing components in the market based on requirements for an 800 tons OKBC and analyzing the SCC mass properties, it was found that mounting the high-power SCC' drive unit on the cylinder might not be the best option for high-power OKBCs. Therefore, an alternative way of deploying the SCC drive unit needs to be explored. Consequently, this paper contributes to addressing gaps as follows:

- The 800 tons OKBC cylinder parameters are analyzed and calculated according to the maximum load, speed, and pressure limits. The main components of the knuckle boom 1M1P SCC with 3200 tons load capacity are selected from commercial products based on the cylinder parameters.
- A commercial 150 tons OKBC was modeled in Simulink based on data from the industrial partner. The operating range of the crane yoke was identified and plotted. A four-quadrant operating trajectory for lifting a 20 tons tubular load was developed by using the spline function.
- Two 1M1P SCC driving the MBC and KBC were modeled based on commercial products' datasheets. Two ways of deploying the SCC' drive unit, compact and remote deployment, on the 150 tons OKBC were modeled and compared. Compact deployment is mounting the SCC drive unit on the cylinder. Remote deployment is mounting the SCC drive unit in the crane machine room.
- Compared with Compact deployment, a maximum of 6.2 % MBC output power can be saved by remote deployment in the planned operating condition. If maintaining the same MBC SCC pump power as in Compact deployment, the tubular load can be increased by 30.5 % in remote deployment.
- The long pipelines used in remote deployment only cause 0.4 % peak power loss and have no significant influence on tracking performance.

For these reasons, high-power 1M1P-SCCs can be constructed with off-shelf commercial products from the market for the 800 tons offshore hydraulic knuckle boom crane. Furthermore, mounting the SCC drive unit in the machine room is superior to mounting the SCC drive unit on the hydraulic cylinder for high-power offshore hydraulic knuckle boom cranes in terms of power consumption and load capacity.

6.2 Future work

There are different types of SCCs in terms of how many electric motors and hydraulic pumps are used, such as 1M1P, one-motor-two-pump, and two-motor-two-pump SCCs. Different types of SCC weigh differently at the same power level. In this paper, only the 1M1P SCC is numerically investigated. For comprehension, other types of SCC should be investigated in future work. Furthermore, only one load case and one operating path are considered in the simulation. Other load cases and operating paths should also be investigated to enhance the conclusion. In simulations, the long pipeline in remote deployment does not affect the control performance. It is because the control inputs are moderate. In future work, harsh control inputs should be used to investigate the pipeline influence on the system control performance, and more advanced controllers should be designed if significant influences are found. Energy recuperation under overrunning load is not considered in this paper. Therefore, the SCC drive unit weight in compact deployment only consumes power in operations.

Another solution for addressing the challenges mentioned in Sec. 2.3 is that the accumulators can be replaced with a low-pressure booster pump circuit. This solution can reduce the system's weight, as the accumulator's weight is higher than the booster pump circuit. However, this solution needs detailed evaluation regarding the feasibility of the hydraulic circuit and the decrease in efficiency of the system. Therefore, using a booster pump circuit can be the future scope of the study.

Nomenclature

Acronyms	Denotation		Acronyms	Denotation	
KBC	Knuckle boom cylinder		SCC	Speed-controlled hydraulic cylinder	
1M1P	One-motor-one-pump		MBC	Main boom cylinder	
OKBC	Offshore knuckle boom crane		POCV	Pilot-operated check valve	
ISV	Invert shuttle valve				
Symbols	Denotation	Unit	Symbols	Denotation	Unit
n_m	Motor speed	rev/min	n_{comd}	Motor speed command	rev/min
ω_m	Motor eigenfrequency	rad/s	ζ_m	Motor damping ratio	-
Q_p	Pump flow rate	L/min	V_p	Pump displacement	cm^3/rev
k_{air}	Air adiabatic constant	-	β_{chb}	Chamber oil bulk modulus	bar
β_{oil}	Standard oil bulk modulus	bar	$\beta_{chb,air}$	Chamber Entrapped air bulk modulus	bar
p_{chb}	Chamber pressure	bar	p_{atm}	Atmospheric pressure	bar
$V_{atm,\%air}$	Entrapped air relative volume when oil in open air	-	$V_{chb,\%air}$	Entrapped air relative volume in chamber oil	-
p_1	Piston side chamber pressure	bar	p_2	Rod side chamber pressure	bar
p_3	Accumulator pressure	bar	Q_{pis}	Piston side flow rate	L/min
Q_{rod}	Rod side flow rate	L/min	v_{rod}	Rod velocity	m/s
x_{rod}	Rod position	m	x_{end}	Cylinder stroke end	m
x_{lim}	Cylinder stroke limits	m	A_{pis}	Piston area	m^2
A_{rod}	Rod area	m^2	A_{annu}	Annular area	m^2
V_0	Pipeline and dead volume	m^3	F_{cyl}	Cylinder force	N
F_{cont}	Contact force between the piston and the cylinder	N	k_{cont}	Contact spring constant	N/m
c_{cont}	Contact damping coefficient	N·s/m	F_f	Friction force	N
f_v	Viscous friction coefficient	N·s/m	γ	Hyperbolic tangent coefficient	-
F_C	Coulomb friction force	N	F_S	Static friction force	N
τ	Static friction time constant	-	$Q_{rv,pis}$	Piston side relief valve flow rate	L/min
$Q_{rv,rod}$	rod side relief valve flow rate	L/min	$p_{crk,rv}$	Valve cracking pressure	bar
k_{rv}	Relief valve flow rate coefficient	L/min/bar	$Q_{pocv,pis}$	Piston side POCV flow rate	L/min
$Q_{pocv,rod}$	Rod side POCV flow rate	L/min	C_d	Orifice discharge coefficient	-
$u_{pocv,pis}$	Piston side POCV opening	-	$u_{pocv,rod}$	Rod side POCV opening	-
$u_{comd,pis}$	Piston side POCV opening command	-	$u_{comd,rod}$	Rod side POCV opening command	-
Ψ	POCV Pilot ratio	-	$p_{crk,pocv}$	POCV cracking pressure	bar
k_{pocv}	POCV maximum opening pressure	bar	ω_{pocv}	POCV eigenfrequency	rad/s
ζ_{pocv}	POCV damping ratio	-			

References

[1] J. D. Zimmerman, M. Pelosi, C. A. Williamson, and M. Ivantysynova. Energy consumption of an ls excavator hydraulic system. In *Proceedings of ASME 2007 International Mechanical Engineering Congress and Exposition*, pages 117–126, Seattle, Washington, USA, 2007.

[2] S. Qu, D. Fassbender, A. Vacca, and E. Busquets. A high-efficient solution for electro-hydraulic actuators with energy regeneration capability. *Energy*, page 119291, 2020.

[3] S. Ketelsen, D. Padovani, T. O. Andersen, M. K. Ebbesen, and L. Schmidt. Classification and review of pump-controlled differential cylinder drives. *Energies*, 12:1–27, 2019.

[4] W Zhao, M K Ebbesen, and T O Andersen. Identifying the future research trend for using speed-controlled hydraulic cylinders in offshore applications through literature survey. In *Proceedings of 2022 IEEE Global Fluid Power Society PhD Symposium (accepted)*, Naples, Italy, 2022.

[5] J. Weber, B. Beck, E. Fischer, G. Kolks, J. Lübbert, S. Michel, M. Schneider, R. Ivantysyn, L. Shabi, M. Kunkis, A. Sitte, H. Lohse, and J. Weber. Energy consumption of an ls excavator hydraulic system. In *Proceedings of The 10th International Fluid Power Conference*, pages 29–62, Dresden, Germany, 2016.

[6] S. Frischemeier. Electrohydrostatic actuators for aircraft primary flight control-types, modelling and evaluation. In *Proceedings of the Fifth Scandinavian International Conference on Fluid Power*, pages 1–16, Linköping, Sweden, 1997.

[7] D. Hagen, D. Padovani, and M. Choux. A comparison study of a novel self-contained electro-hydraulic cylinder versus a conventional valve-controlled actuator-part 1: Motion control. *Actuators*, 8, 2019.

[8] D. Hagen, D. Padovani, and M. Choux. A comparison study of a novel self-contained electro-hydraulic cylinder versus a conventional valve-controlled actuator-part 2: Energy efficiency. *Actuators*, 8, 2019. Read in 20.10.2020.

[9] K. G. Cleasby, A. R. Plummer, and T. Company. A novel high efficiency electrohydrostatic flight simulator motion system. In *Proceedings of ASME/BATH 2008 Symposium on Fluid Power and Motion Control*, pages 437–449, Bath, UK, 2008.

[10] S. Zhang, T. Minav, and M. Pietola. Decentralized hydraulics for micro excavator. In *Proceedings of 15th Scandinavian International Conference on Fluid Power*, pages 187–195, Linköping, Sweden, 2017.

[11] E. Siemer. Variable-speed pump drive system for a 5000 kN ring expander. In *Proceedings of 8th International Fluid Power Conference*, Dresden, Germany., 2012.

[12] S. Ketelsen, T. O. Andersen, M. K. Ebbesen, and L. Schmidt. A self-contained cylinder drive with indirectly controlled hydraulic lock. *Modeling, Identification and Control: A Norwegian Research Bulletin*, 41:185–205, 2020.

[13] S. H. Cho and S. Helduser. Robust motion control of a clamp-cylinder for energy-saving injection moulding machines. *Journal of Mechanical Science and Technology*, 22:2445–2453, 2008.

[14] S. Helduser. Electric-hydrostatic drive-an innovative energy-saving power and motion control system. *Proceedings of the Institution of Mechanical Engineers, Part I: Journal of Systems and Control Engineering*, 213:427 – 437, 1999.

[15] S. HELDUSER. Electric-hydrostatic drive systems and their application in injection moulding machines. In *Proceedings of the JFPS International Symposium on Fluid Power, 1999*, pages 261–266, Japan, 1999.

[16] Parker Hannifin. Compact eha-electro-hydraulic actuators for high power density applications. [EB/OL]. `https://www.parker.com/Literature/Hydraulic%20Pump%20Division/Oildyne%20EHA/Compact-EHA-Catalog-HY22-3101E-7-13.pdf` Accessed October 7, 2022.

[17] Bosch Rexroth AG. Servo-hydraulic actuator - sha fields of application. [EB/OL]. `https://www.boschrexroth.com/documents/12605/25201122/RE_08137_2021-04.pdf/e4082d77-4692-3e55-3a02-5a6e0d2ea568?routed=true` Accessed October 7, 2022.

[18] Servi Group. Servi hybrid drive. [EB/OL]. `https://www.servi.no/media/atfckla5/servi-hybrid-drive-en-low.pdf` Accessed October 7, 2022.

[19] S. Ketelsen, T. O. Andersen, M. K. Ebbesen, and L. Schmidt. Mass estimation of self-contained linear electro-hydraulic actuators and evaluation of the influence on payload capacity of a knuckle boom crane. In *Proceedings of ASME/BATH 2019 Symposium on Fluid Power and Motion Control*, Longboat Key, Florida, USA., 2019.

[20] National Oilwell Varco. Lifting & handling product portfolio. [EB/OL]. `https://www.nov.com/-/media/nov/files/products/rig/lifting-and-handling-product-portfolio.pdf` Accessed Nov. 4, 2022.

[21] S. Ketelsen, T. O. Andersen, M. K. Ebbesen, and L. Schmidt. A self-contained cylinder drive with indirectly controlled hydraulic lock. *Modeling, Identification and Control: A Norwegian Research Bulletin*, 41:185–205, 2020.

[22] Epe Italiana Srl. Hydropneumatic accumulators and components. [EB/OL]. `https://www.epeitaliana.it/wp-content/uploads/2020/06/Catalogo-Generale-EPE-2019.pdf` Accessed Nov. 4, 2022.

[23] Bosch rexroth. Axial piston variable pump a4vso. [EB/OL]. https://www.boschrexroth.com/da/dk/produkter/produktgrupper/mobilhydraulik/pumps/axial-piston-pumps/variable-pumps-open-circuit/a4vso Accessed Nov. 4, 2022.

[24] HYDAC. Accumulator technology. product catalogue. [EB/OL]. http://hydac.com.sg/wp-content/uploads/2018/08/accumulator-full-catalogue.pdf Accessed Nov. 4, 2022.

[25] J. Watton. *Fundamentals of Fluid Power Control*. Cambridge University Press, 2009.

[26] G. K. Costa and N. Sepehri. Four-quadrant analysis and system design for single-rod hydrostatic actuators. *Journal of Dynamic Systems, Measurement and Control, Transactions of the ASME*, 141:1–15, 2019.